BOREAS An international journal of Quaternary research

Past millennium hydroclimate variability from Corsican pine tree-ring chronologies

JAN ESPER, CLAUDIA HARTL, OLIVER KONTER, FREDERICK REINIG, PHILIPP RÖMER, FRÉDÉRIC HUNEAU, SEBASTIEN LEBRE, SONJA SZYMCZAK, ACHIM BRÄUNING AND ULF BÜNTGEN

BOREAS

Esper, J., Hartl, C., Konter, O., Reinig, F., Römer, P., Huneau, F., Lebre, S., Szymczak, S., Bräuning, A. & Büntgen, U.: Past millennium hydroclimate variability from Corsican pine tree-ring chronologies. *Boreas*. https://doi.org/10.1111/bor.12574. ISSN 0300-9483.

Palaeoclimatic evidence is necessary to place the current warming and drying trends of the Mediterranean region in a long-term perspective of pre-industrial variability. Annually resolved and absolutely dated climate proxies that extend back into medieval times are, however, limited to a few sites only. Here we present a network of long ring width chronologies from *Pinus nigra* tree-line sites in northern Corsica (France) that cohere exceptionally well over centuries and support the development of a single high-elevation pine chronology extending back to 974 CE. We apply various detrending methods to these data to retain high-to-low frequency ring width variability and scale the resulting chronologies against instrumental precipitation and drought observations to produce hydroclimate reconstructions for the last millennium. Proxy calibration and transfer are challenged by a lack of high-elevation meteorological data, however, limiting our understanding of precipitation changes in sub-alpine tree-line environments. Our new reconstructions extend beyond existing records and provide evidence for low-frequency precipitation variability in the central-western Mediterranean from 974–2016 CE. Comparison with a European scale drought reconstruction network shows that regional predictor chronologies are needed to accurately estimate long-term hydroclimate variability on Corsica.

Jan Esper (esper@uni-mainz.de), Department of Geography, Johannes Gutenberg University, 55099 Mainz, Germany and Global Change Research Institute of the Czech Academy of Sciences (CzechGlobe), 60300 Brno, Czech Republic; Claudia Hartl, Oliver Konter, Frederick Reinig and Philipp Römer, Department of Geography, Johannes Gutenberg University, 55099 Mainz, Germany; Frédéric Huneau, Faculty of Science and Technology, University of Corsica Pasquale Paoli, 20250 Corte, France and National Centre for Scientific Research, UMR 6134, SPE, 20250 Corte, France; Sebastien Lebre, National Forest Office, 20250 Corte, France; Sonja Szymczak and Achim Bräuning, Institute of Geography, Friedrich-Alexander University Erlangen-Nürnberg, 91058 Erlangen, Germany; Ulf Büntgen, Department of Geography, University of Cambridge, Cambridge, CB2 3EN, UK and Department of Geography, Faculty of Science, Masaryk University, 61300 Brno, Czech Republic and Swiss Federal Research Institute WSL, 8903 Birmensdorf, Switzerland and Global Change Research Institute of the Czech Academy of Sciences (CzechGlobe), 60300 Brno, Czech Republic; *received 28th July 2021, accepted 12th November 2021.*

The reconstruction of high-resolution climate variability beyond the period covered by meteorological station data is needed to place current Mediterranean dynamics into a long-term context and compare anthropogenically forced with natural climate variations (Luterbacher 2012). Several tree-ring based temperature and hydroclimate studies have been reported from the central Mediterranean including chronologies derived from broadleaf and conifer networks in central and southern Italy (Leonelli *et al.* 2017) and southeastern France (Lebourgeois *et al.* 2012). The Italian network includes tree-ring maximum latewood density (MXD) data that have been used to produce an August–September temperature reconstruction extending back to 1714 CE, revealing colder conditions in the 1810s preceded by a warmer period in the late 18th century (see also Briffa *et al.* 1998). Leonelli *et al.* (2017) also analysed tree-ring width (TRW) data and report widespread sensitivity of Italian conifers to drought conditions that occurred 1 year prior to the formation of the actual ring (hereafter: previous-year signal). The network analysis from southeastern France (Lebourgeois *et al.* 2012) revealed varying and temporally instable climate signals in deciduous and conifer trees, though the 67 TRW site chronologies included in their study were only weakly replicated (n_{avg} = 4.5 series per site). TRW chronologies from high-elevation *Pinus nigra* sites >1200 m a.s.l. in Mediterranean France showed significant correlations with current-year May and June precipitation, however. The French and Italian networks are framed by longer tree-ring based temperature and hydroclimate reconstructions from Spain in the west and the Balkans down to Greece in the east (Griggs *et al.* 2007; Büntgen *et al.* 2010a, 2012, 2017; Castagneri *et al.* 2014; Trouet 2014; Esper *et al.* 2015a, 2020a; Klesse *et al.* 2015; Seim *et al.* 2015; Tejedor *et al.* 2016, 2017a, b), some of which extend back into the first millennium CE (Seim *et al.* 2012; Klippel *et al.* 2018, 2019; Esper *et al.* 2020b, 2021), demonstrating the significance of pre-instrumental climate variability frequently exceeding the variance recorded during the Anthropocene. Most of these studies report difficulties in properly calibrating TRW and MXD data from sub-alpine Mediterranean sites as a consequence of steep hydroclimatic gradients in high mountain

DOI 10.1111/bor.12574

environments and lack of tree-line meteorological station data. This limitation is particularly striking for precipitation readings from high-elevation Mediterranean environments (Knerr *et al*. 2020).

Corsica, as one of the most mountainous islands in the Mediterranean, has been focused upon in several dendroclimatic studies analysing the sensitivity of TRW, MXD and stable isotope measurements to temperature and hydroclimate variability (Hetzer 2013; Häusser *et al*. 2019; Szymczak *et al*. 2019, 2020b). Whereas measurements of tree-ring stable carbon isotopes from high-elevation *Pinus nigra* have been used to reconstruct August–September temperatures back to 1448 CE (Szymczak *et al*. 2012), recent work on MXD data from Corsican pines revealed temporally changing climate signals in this classic proxy (Römer *et al*. 2021). A combined record of TRW data from a network of 15 *Pinus nigra* sites has been used to reconstruct summer (June–August) precipitation back to 1185 CE (Szymczak *et al*. 2014). This reconstruction is constrained to high-frequency, interannual to decadal scale precipitation variability, as the TRW series included in this record were detrended using flexible spline highpass filters to remove tree-age related noise from the data. TRW data from a *Pinus nigra* site at 1400 m a.s.l. on the Corsican Col de Sorba, published in an earlier study (Schweingruber & Briffa 1996), were also used in a large-scale tree-ring network to produce gridded reconstructions of the Palmer Drought Severity Index (PDSI; van der Schrier *et al*. 2013) covering Europe at a resolution of $0.5° \times 0.5°$ over the past two millennia (Cook *et al*. 2015). This European drought atlas enables the comparison of Anthropocene drought dynamics with pre-instrumental variations back to Medieval and even Roman times at regional (e.g. Corsican) scales.

We here acknowledge these important attempts to reconstruct regional climate variability beyond the period covered by meteorological station data and present a network of new and updated high-elevation TRW chronologies from four Corsican valleys. The chronologies include hundreds of TRW series from living and relict pines from sub-alpine environments >1400 m a.s.l. reaching back over the past eight to eleven centuries. We assess the covariance among these long TRW site chronologies and compare mean curves of all data with precipitation totals and the PDSI derived from local meteorological stations. This is done considering differently detrended TRW chronologies to evaluate the possibility of reconstructing high-to-low frequency hydroclimate variability, including multidecadal to centennial scale trends, throughout the past millennium. The precipitation and PDSI reconstructions derived from this work are finally compared with existing records from Corsica and the European drought atlas with focus on changing covariances back in time.

Material and methods

Study sites and TRW chronologies

Four high-elevation *Pinus nigra* sites in the Asco, Ballone, Golo and Tartagine valleys have been visited during three field campaigns since 2017 (Fig. 1). The sites are all located >1400 m a.s.l. in steep environments near the upper tree line where Corsican pine is the dominating tree species reaching ages >800 years (Table 1). These old-growth sub-alpine sites are characterized by a sparse vegetation cover on partly shallow soils from alkaline granites, influenced by episodic fire disturbances (Szymczak *et al*. 2020a).

We collected a total of 681 core and disc samples from 412 living trees and dry-dead stumps on the ground. The Asco and Ballone sites are better replicated (285 and 269 radii, respectively) as the trees appeared to be older and more stumps were found. The samples were polished and cut to make tracheids and ring boundaries visible, and TRW was measured at an accuracy of 0.01 mm to produce a dataset including almost 200 000 values.

Average growth rate of Corsican tree-line pines is fairly low, ranging from 0.83 mm a^{-1} in Tartagine to 1.13 mm a^{-1} in Asco. These minor growth rate differences are affected by variable mean tree ages ranging from 260 years in Ballone to 342 in Tartagine. The growth curves of the age-aligned data are highly similar among the sites (Fig. S1), however, supporting the combination of data without adjustments (Esper *et al*. 2014). Inter-series correlations (Rbar in Table 1) range from 0.32 to 0.44 revealing successful cross-dating and substantial environmental forcing (Holmes 1983), and the combined living-tree plus relict-wood site chronologies extend back to the 12th (Golo and Tartagine) and 10th centuries (Asco and Ballone).

The 681 TRW series were detrended using varying spline highpass filters (Cook & Peters 1981) to emphasize high-to-low frequency variance in the resulting mean chronologies and evaluate different levels of spline detrending in search of an optimal choice for climate reconstruction (Blasing *et al*. 1983; Briffa 1984). We considered 10-year, 30-year, 100-year, 500-year and 1000-year splines (hereafter 10sp, 30sp, ... 1000sp) fitted to the power transformed TRW series (Cook & Peters 1997), calculated residuals between the measurement series and splines, and computed mean chronologies using the biweight robust mean. This was done to produce TRW site chronologies for each of the four alpine valleys Asco, Ballone, Golo and Tartagine (Fig. 2), as well as a Corsican high-elevation pine chronology (CHEPI) integrating the data from all sites. Due to the varying site replications (radii in Table 1), the Asco and Ballone valleys are overrepresented in the CHEPI chronology. All chronologies were variance-adjusted by calculating ratios from 300-

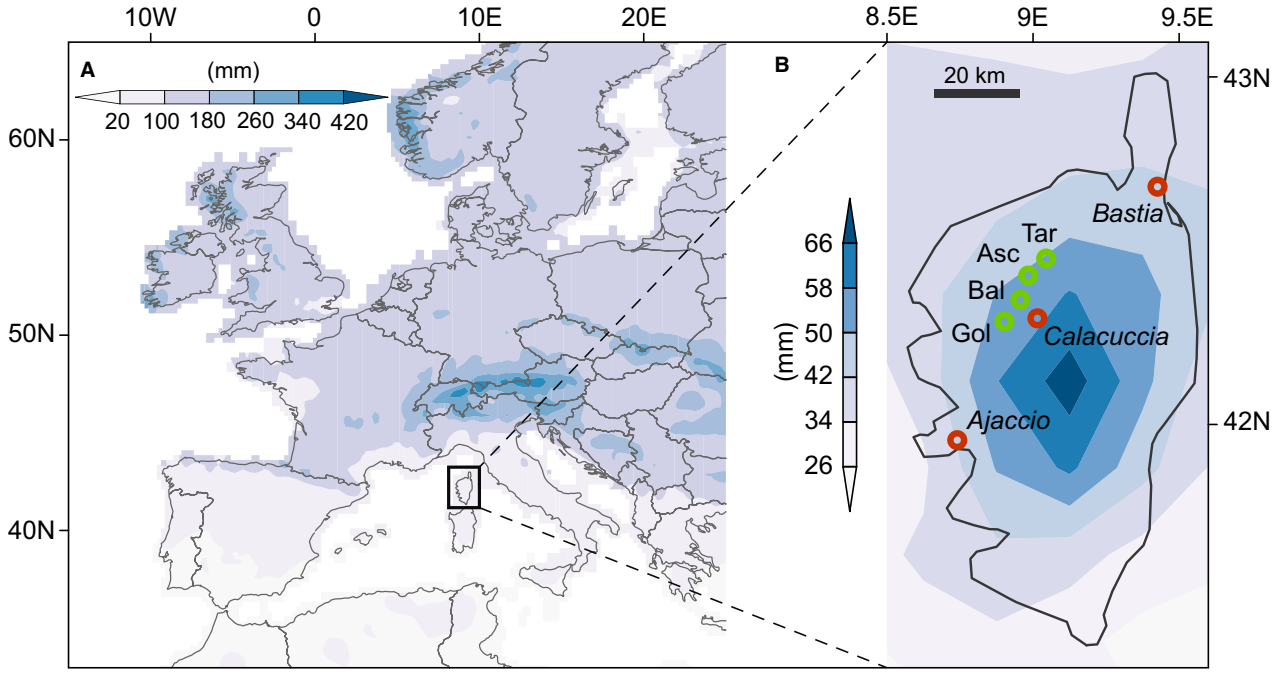

Fig. 1. Map showing the location of Corsica in Europe (A), and the tree-ring sampling sites (green) and meteorological stations (red) on the island (B). Contours indicate June–July precipitation totals ranging from <20 to >420 mm in Europe and from <26 to >66 mm in Corsica derived from GPCC gridded data (Schneider *et al.* 2021).

year splines fitted to absolute chronology departures to account for changes in sample replication and covariance through time (Frank *et al.* 2007).

Instrumental climate data and adjustment

We used Corsican meteorological station records as well as gridded precipitation, temperature and PDSI data to evaluate the climate signals in the pine TRW chronologies. Corsica hosts several climate stations extending back over 60 years, one of which at 875 m a.s.l. (Calacuccia) is near the studied tree sites, and two longer records at 5 and 10 m a.s.l. (Ajaccio and Bastia), respectively (Fig. 1B). Ajaccio and Bastia are situated at the drier coastline, compared to the high-elevation station in Calacuccia recording 892 mm a^{-1}. However, none of the records mirrors the moist conditions at the pine tree-line sites above 1400 m a.s.l. where annual precipitation is estimated to exceed 1500 mm, of which ~80% is estimated to fall from October–April (Hetzer 2013; Knerr *et al.* 2020).

The Corsican climate stations show characteristic Mediterranean seasonal patterns including distinct summer precipitation deficits and minima in July: 16 mm in Calacuccia, 12 mm in Bastia, 7 mm in Ajaccio (1981–2010 CE). Monthly precipitation totals recorded at the Calacuccia high-elevation station correlate only moderately with the low-elevation data, reaching a minimum of only $r = 0.29$ with June precipitation recorded in Ajaccio from 1962–2016 CE (Fig. 3B), thereby demonstrating substantial precipitation heterogeneity particularly during the summer months. This lack of spatial representation is also seen in the GPCC (Schneider *et al.* 2021) and CRU (Harris *et al.* 2020) gridded products, when correlating station precipitation with grid point data at latitude 9.125E/42.125N (GPCC), longitude 9.25E/42.25N (CRU) near the pine tree-ring sites (Fig. 3B). These comparisons demon-

Table 1. TRW site chronology characteristics. *Age refers to the arithmetic mean of all radii. AGR is the average growth rate in mm a^{-1}. Rbar is the inter-series correlation among radii.

Site	Code	Elevation (m a.s.l.)	Lat.	Lon.	Trees	Radii	Age*	AGR*	Rbar*	Period
Asco	Asc	1600–1700	42.40	8.92	173	285	276	1.13	0.32	948–2017
Ballone	Bal	1520–1700	42.35	8.91	180	269	260	0.92	0.41	962–2017
Golo	Gol	1410–1550	42.31	8.87	31	66	293	1.05	0.37	1173–2017
Tartagine	Tar	1440–1515	42.46	8.94	28	61	342	0.83	0.44	1143–2016

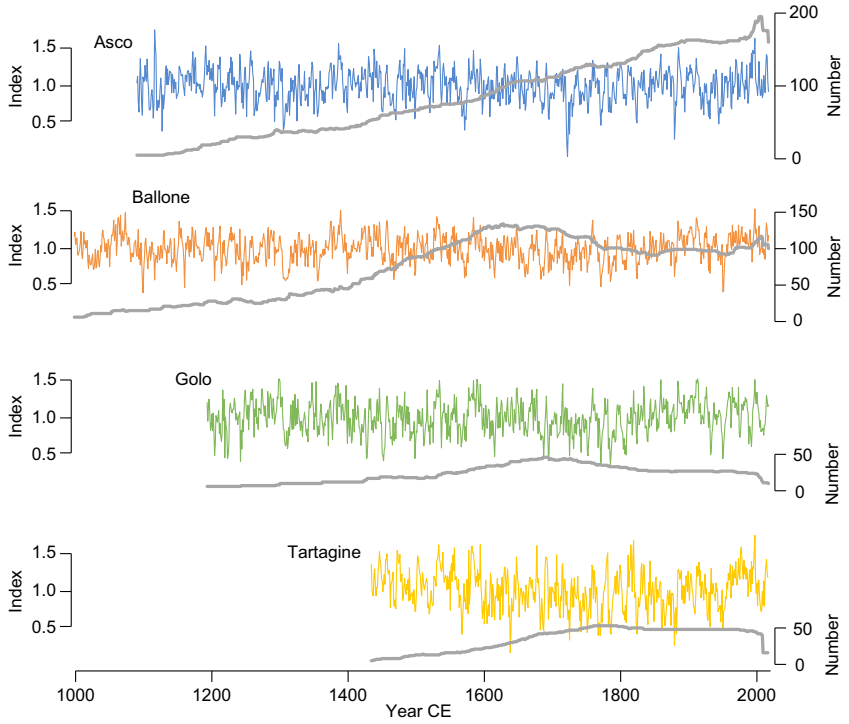

Fig. 2. 1000-year spline detrended TRW chronologies from high-elevation *Pinus nigra* sites in the Asco, Ballone, Golo and Tartagine valleys together with their corresponding replication curves (grey).

strate a reduced covariance between high-elevation Calacuccia and CRU data (as Calacuccia is not included in this product), and more generally, between the station records and gridded data particularly during the dry summer months.

The drier conditions at the Corsican meteorological stations, compared to the pine tree-line sites, and the low correlations between station and gridded data limit the reliability of observational data to successfully calibrate TRW data recorded at elevations >1400 m a.s.l. This limitation is accentuated during summer as spatial correlation fields are substantially smaller than during winter (Fig. 3D), and because the summer month time series frequently include zero precipitation (Fig. 3E), which biases correlation-based calibration trials. These problems are substantially reduced with temperature, as the monthly thermometer readings correlate much better over larger distances (Büntgen *et al.* 2010b) and along elevational transects (Knerr *et al.* 2020). Yet derived drought indices, such as the PDSI (van der Schrier *et al.* 2013), that rely on the same observations, contain similar deficiencies as detailed here for precipitation (Fig. S2).

To account for the reduced absolute precipitation values in the Corsican station network, the observational data were adjusted to approximate the conditions at the four tree-line sites in Asco, Ballone, Golo and Tartagine at an average elevation of 1560 m a.s.l. Considering the annual precipitation totals recorded in Ajaccio (598 mm), Bastia (799 mm) and Calacuccia (892 mm), as well as a shorter record from a high-elevation station in Evisa (1438 mm at 1030 m a.s.l.), we derived a lapse rate of 53 mm per 100 m from linear regression. Considering this lapse rate, annual precipitation at 1560 m a.s.l. is estimated to equal 1510 mm, whereas the actual mean of the three station records in Ajaccio, Bastia and Calacuccia employed here for calibration is only 760 mm. We therefore adjusted the mean station precipitation totals by essentially doubling (+99%) the monthly values before using these data to transfer TRW chronologies. No such adjustments were applied when using the self-calibrated PDSI for transfer as these data fluctuate at a normalized scale around zero (van der Schrier *et al.* 2013).

Proxy calibration and transfer

Monthly mean time series of the station records from Ajaccio, Bastia and Calacuccia back to 1962 CE for precipitation (hereafter ABC_P) and 1947 CE for temperature (ABC_T) were used for calibration of differently detrended (10sp–1000sp) CHEPI chronologies. For precipitation, we additionally used gridded GPCC data to evaluate climate signals back to 1891 CE. For drought, we used the gridded self-calibrated PDSI from 1947–2016 CE covered by Corsican station temperature data, as well as back to 1901 CE covered by remote station data to study signal strength changes over earlier

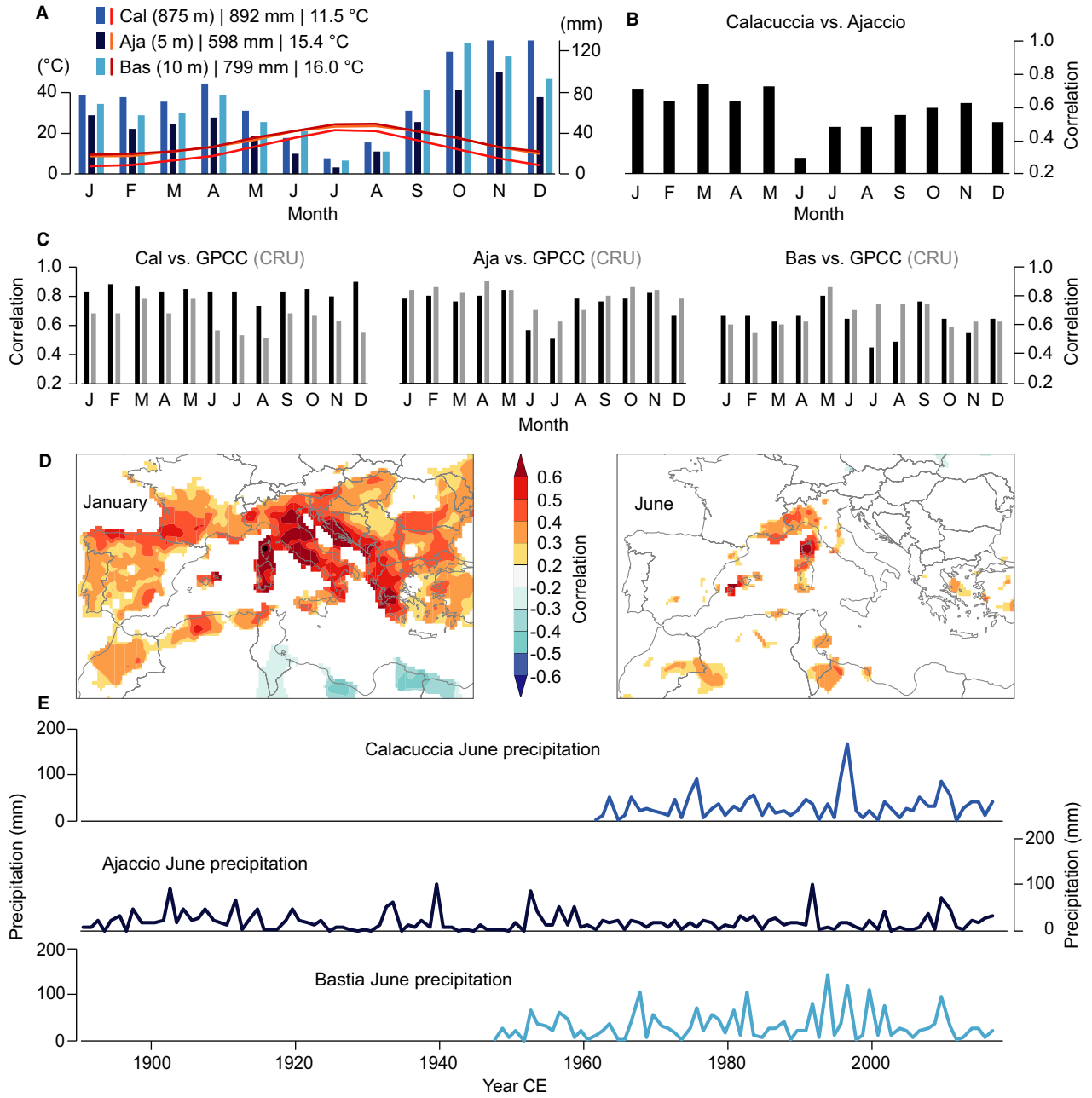

Fig. 3. Meteorological data. A. Climate diagram of the meteorological stations in Calacuccia (Cal), Ajaccio (Aja) and Bastia (Bas) averaging temperatures (red curves) and precipitation (blue bars) from 1981–2010 CE. B. Correlations between monthly precipitation totals recorded in Calacuccia and Ajaccio from 1962–2016 CE. C. Same as in (B), but for Calacuccia, Ajaccio and Bastia vs. GPCC (black) and CRU (grey) precipitation from nearby grid points at 9.125E/42.125N and 9.25E/42.25N, respectively. D. Spatial correlation patterns of precipitation recorded in Calacuccia against the GPCC grid for January (left) and June (right) from 1962–2016 CE. E. June precipitation recorded in Calacuccia (since 1962 CE), Ajaccio (1891) and Bastia (1948).

periods. The relationship between CHEPI chronologies and monthly observational data, from previous-year March to current-year October, was assessed using Pearson product-moment correlations. For precipitation, we additionally considered Spearman rank correlations to account for the exceptionally dry summer months and compare the coefficients of the two methods.

To transfer the proxy data into estimates of hydroclimate variability, the differently detrended CHEPI chronologies were scaled (Esper *et al.* 2005) against previous-year and current-year warm season precipitation data from ABC_P, as well as previous-year September PDSI data from the 9.125E/42.125N grid point. Transfer models were assessed considering the reduction of error

(RE) and coefficient of efficiency (CE) statistics derived from CHEPI chronologies regressed against target precipitation (PDSI) data over the 1962–1988 (1947–1981) and 1989–2016 CE (1982–2016 CE) calibration-verification periods (Cook *et al.* 1994). The Durbin–Watson (DW) statistic was calculated over the 1962–2016 and 1947–2016 CE periods to estimate potential low frequency divergence from ABC_P and PDSI targets, respectively (Durbin & Watson 1951). Whereas RE and CE values >0 indicate predictive skill, DW scores around 2 indicate insignificant trends in proxy-target residuals.

Potential long-term signal strength changes of the millennial-length hydroclimate reconstructions were assessed considering the CHEPI replication curve as well as the running inter-series correlation (Rbar) calculated over 50-year segments combined in the expressed population signal (EPS; Wigley *et al.* 1984). The new reconstructions are finally compared with a summer precipitation record derived from a Corsican pine network back to 1185 CE (Szymczak *et al.* 2014), and a grid point summer PDSI reconstruction from the European drought atlas back to 974 CE (Cook *et al.* 2015).

Results and discussion

TRW covariance

TRW site chronologies are highly similar among the four Corsican mountain valleys (Fig. 4) supporting the combination of data into a single CHEPI record. Inter-site correlations calculated over the 1434–2016 CE common period (583 years) range from $r = 0.68$ for 1000sp chronologies to $r = 0.70$ for 10sp and 100sp chronologies, thereby revealing only minor differences due to changing detrending method (here varying spline stiffness). Inter-site covariance also remains high back in time, as is demonstrated by 50-year running correlations calculated over the past six centuries (Fig. 4B). Whereas some of these correlations temporarily drop below $r = 0.4$ in the 20th and early 18th centuries, the correlation mean persistently exceeds $r = 0.5$. Particularly striking are the $r > 0.6$ values recorded over the early period before 1600 CE, when chronology replication drops, and Golo and Tartagine integrate only a few TRW series (grey curves in Fig. 2; Gol = 17 and Tar = 5 series in 1434 CE). Inter-site chronology correlations in the order of $r = 0.7$ over almost six centuries are towards the top end of TRW network coherence in Europe (Frank & Esper 2005a, b; Esper *et al.* 2007, 2021; Büntgen *et al.* 2010a, 2011b; Carrer *et al.* 2010; Schneider *et al.* 2014; Hellmann *et al.* 2016; Hartl *et al.* 2021) and not only justify data integration among Corsican sub-alpine pine sites, but also point to a common forcing of tree growth as can only be triggered by climate.

Whereas the changing spline detrendings have only minor effects on inter-site covariance, the retained low frequency trends and autocorrelations vary substantially among the 10sp to 1000sp chronologies (Fig. 5). When zooming into the most recent century, as well as the 1725–1825 CE period of high inter-site covariance, values ranging from $r_{1900–2000} = 0.55–0.62$ and $r_{1725–1825} = 0.77–0.84$ are recorded, with no particular order with respect to detrending. Lag-1 autocorrelations, however, increase

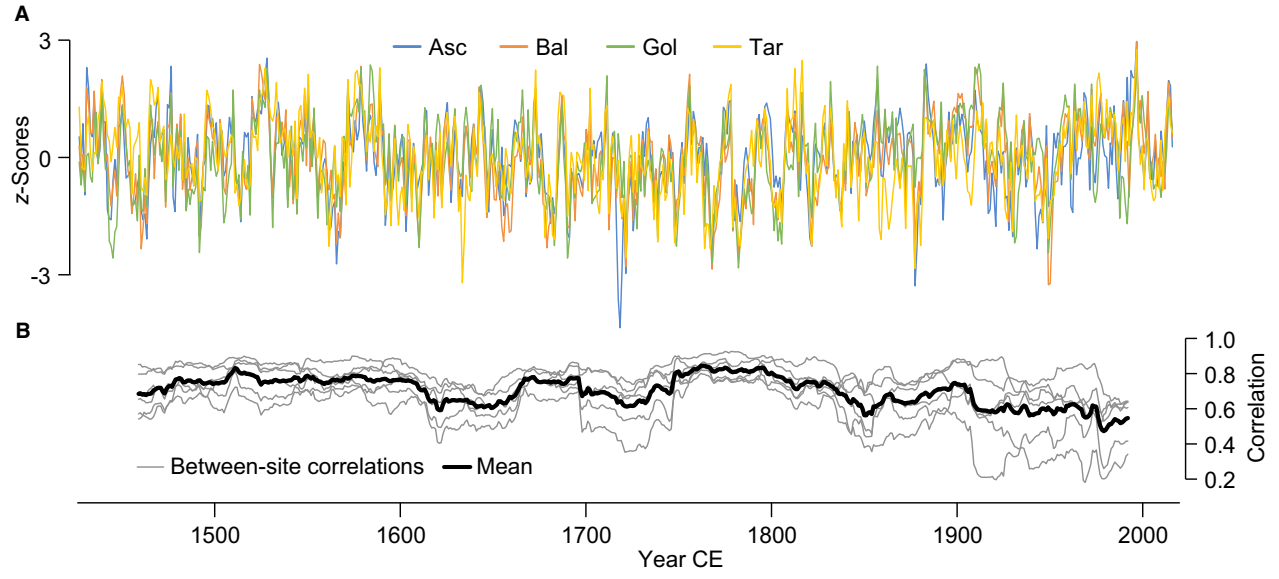

Fig. 4. Inter-site covariance. A. 1000-year spline detrended site chronologies from the Asco, Ballone, Golo and Tartagine valleys back to 1434 CE. B. 50-year running, between-site correlations (thin curves) and their mean (bold curve). All chronologies were transferred into *z*-scores considering the 1962–2016 period.

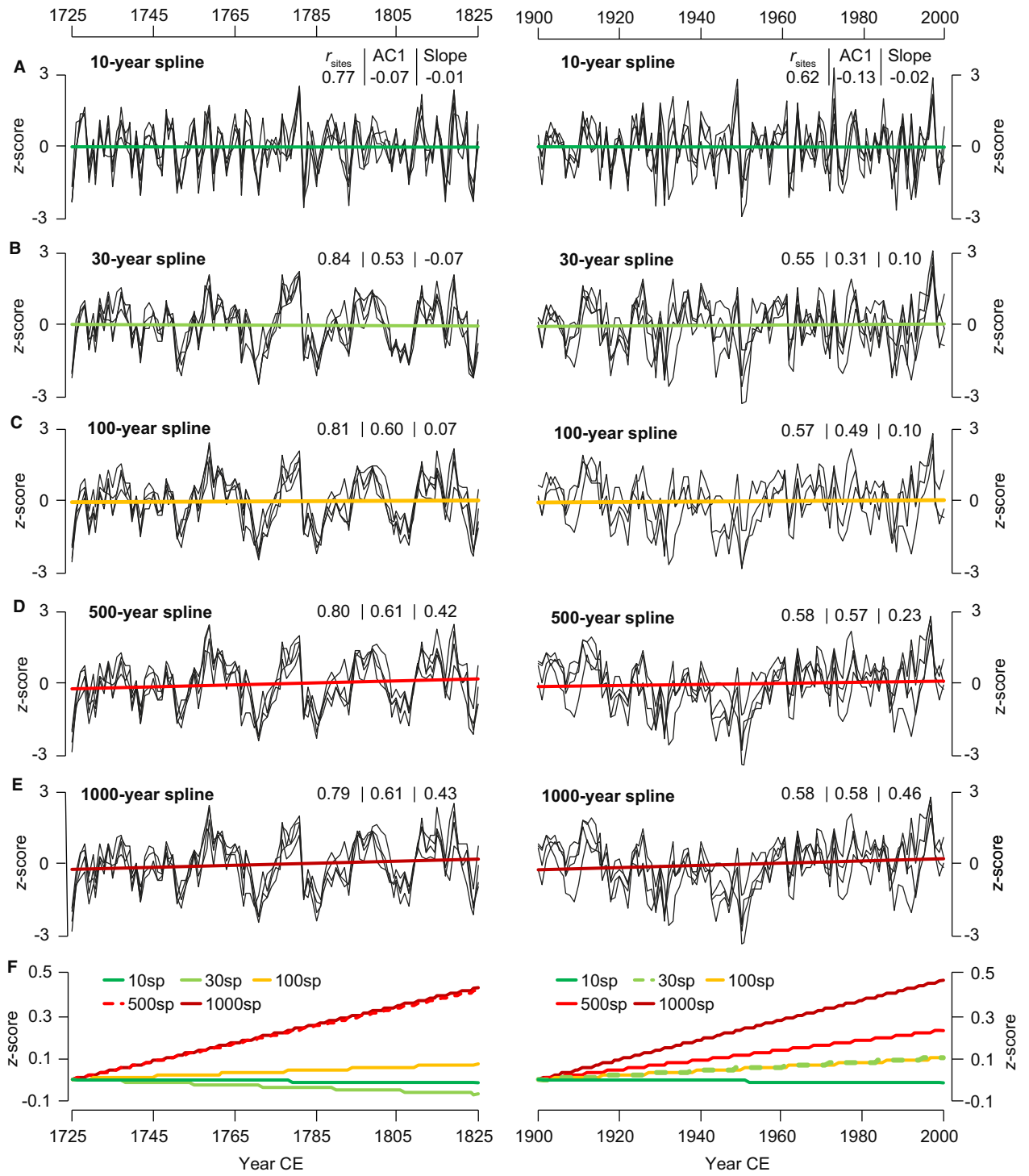

Fig. 5. Covariance and persistence of differently detrended TRW chronologies. A. 10-year spline detrended site chronologies from the Asco, Ballone, Golo and Tartagine valleys (black curves) shown together with a linear regression fit to their mean (green) from 1725–1825 (left) and 1900–2000 CE (right). r_{sites} is the average inter-series correlation among the four site chronologies, AC1 is the average autocorrelation at lag-1 of the site chronologies, and slope is the trend of the linear regression over the 1725–1825 and 1900–2000 CE periods. B–E. Same as in (A), but for the 30sp, 100sp, 500sp and 1000sp detrended TRW data. F. The linear regressions from panels (A–E). All chronologies were normalized over the 1962–2016 period.

from negative values in the 10sp detrended chronologies to $AC1_{1900–2000} = 0.58$ and $AC1_{1725–1825} = 0.61$ in the 1000sp chronologies designed to retain low frequency variance. This latter aspect is emphasized in the linear regressions fit to the chronologies (coloured curves in Fig. 5) demonstrating that the 10sp, 30sp and 100sp

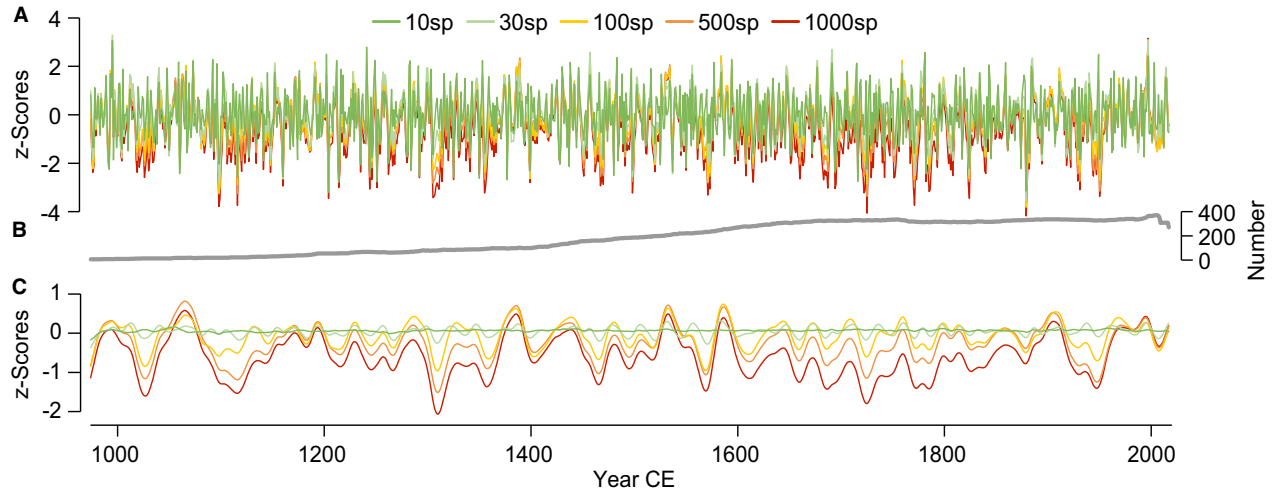

Fig. 6. Corsican high-elevation pine (CHEPI) chronologies. A. CHEPI chronologies derived from 10-year, 30-year, 100-year, 500-year and 1000-year spline detrending shown as *z*-scores with respect to the 1962–2016 period. B. CHEPI replication curve including >5 series after 974 CE, >10 series after 998 CE, and >20 series after 1090 CE. C. 30-year lowpass-filtered chronologies from panel (A).

chronologies contain no substantial centennial-scale trends (slopes < 0.10). The 500sp, and even more so the 1000sp chronologies, on the other hand, contain ample low frequency variance that is largely coherent among the sites. The overall lower inter-site covariance recorded during the 20th century, compared to 1725–1825 CE, could potentially be related to increased human disturbances. Yet the detailed reasons for this weakened network coherence towards present remain unknown.

When sites are combined and the resulting CHEPI chronologies are additionally smoothed, it becomes obvious how the varying detrending methods entirely control the spectra and extremes of potential climate reconstructions derived from these data (Figs 6, S3). Similar effects of tree-ring detrending methodology on retained long-term trends have previously been shown for temperature and hydroclimate reconstructions from other regions in Europe and the Northern Hemisphere (Briffa *et al.* 1992; Esper *et al.* 2002, 2012; D'Arrigo *et al.* 2006; Griggs *et al.* 2007; Fang *et al.* 2010; Büntgen *et al.* 2011a). In Corsica, the coherent inter-site trends indicate that preserving meaningful low frequency variance using stiff splines is feasible, though it remains important to assess the robustness of climate signals among the differently detrended chronologies.

Climate signals

The CHEPI chronologies correlate significantly with monthly precipitation, temperature and PDSI data from Corsican meteorological stations and grid points (see Figs 7, S4 for Spearman rank correlations). The precipitation signal is dichotomous and includes significant correlations with previous-year July–September and current-year June totals, which is in line with *Pinus nigra* TRW signals reported from Italy (Leonelli *et al.* 2017) and Mediterranean France (Lebourgeois *et al.* 2012) including Corsica (Hetzer 2013). The current-year signal extends into high summer, yet the correlations with July precipitation are insignificant ($r < 0.35$). We also found negative precipitation correlations, some of which are stronger in the 30sp and 10sp CHEPI chronologies (light and dark green colours in Fig. 7A), but these inverse relationships are overall weaker compared to the positive correlations. The latter appear physiologically meaningful as warm season precipitation is scarce (Fig. 3) and pine growth benefits from increased soil moisture and lessened stomata closure even in the sub-alpine environments studied here (Häusser *et al.* 2019).

The TRW–temperature correlations partly represent an inversion of the TRW–precipitation pattern, but significant values are only recorded with previous-year months (Fig. 7B). The temperature signal includes several months prior to previous-year September, yet again most of these correlations are insignificant. Given the opposing correlation with previous-year warm season months (positive with precipitation and negative with temperature), it appears challenging to distinguish between truly growth-controlling factors and spurious correlations as moist summers are typically cloudy and cool (Carrer *et al.* 2010). It therefore appears important to recap that the precipitation readings recorded at low-elevation stations are not representative of the conditions at Corsican tree lines. This limitation is particularly important during the dry summer months that include many zero values (Fig. 3E) biasing any correlation-based assessment. With this in mind, the detected precipitation signal is valued more important than the accompanying temperature signal, even though the previous-year September temperature correlation (up to $r_{1947–2016} = -0.57$) is stronger than any of the monthly precipitation correlations (current-year June $r_{1962–2016} = 0.39$).

Fig. 7. Seasonal climate signals. A. Correlations of the differently detrended CHEPI chronologies (colours) with monthly mean precipitation totals of the Ajaccio, Bastia and Calacuccia stations (ABC_P) from 1962–2016. Results from previous-year March (M_P) to current-year October (O) are shown. B. Same as in (A) but for monthly station temperatures (ABC_T) from 1947–2016. C. Same as in (B), but for monthly PDSI data (grid point at 9.25E and 42.25N). $p < 0.01$ reached at $r \approx 0.35$ for the shorter 1962–2016 CE period and at $r \approx 0.31$ for the longer 1947–2016 CE period, considering data autocorrelation.

While it remains tricky to differentiate between original and spurious temperature and precipitation correlations, this obstacle vanishes when considering PDSI data for calibration, as this drought index integrates both temperature and precipitation readings (van der Schrier *et al.* 2013). As a consequence, and due to the in-built memory, several previous-year monthly PDSI time series correlate significantly with CHEPI TRW chronologies, with the highest values reached for previous-year September ($r_{1947–2016} = 0.53$). Almost all monthly correlations show a decrease from the 1000sp to the 10sp chronologies (red and green colours in Fig. 7C) indicating coherent low frequency variance between TRW and drought data and reinforcing the strength of chronologies derived from detrending using stiff splines.

Extended calibration

The CHEPI chronologies were compared with previous-year July–September and current-year June–July (JAS_P&JJ) precipitation, estimated to equal 281 mm (1991–2010 CE) considering the elevational lapse rate detailed above. This was done over the 1962–2016 CE period covered by local station data, including Calacuccia at 875 m a.s.l., as well as over an extended period back to 1891 CE covered by gridded GPCC data (Fig. 8).

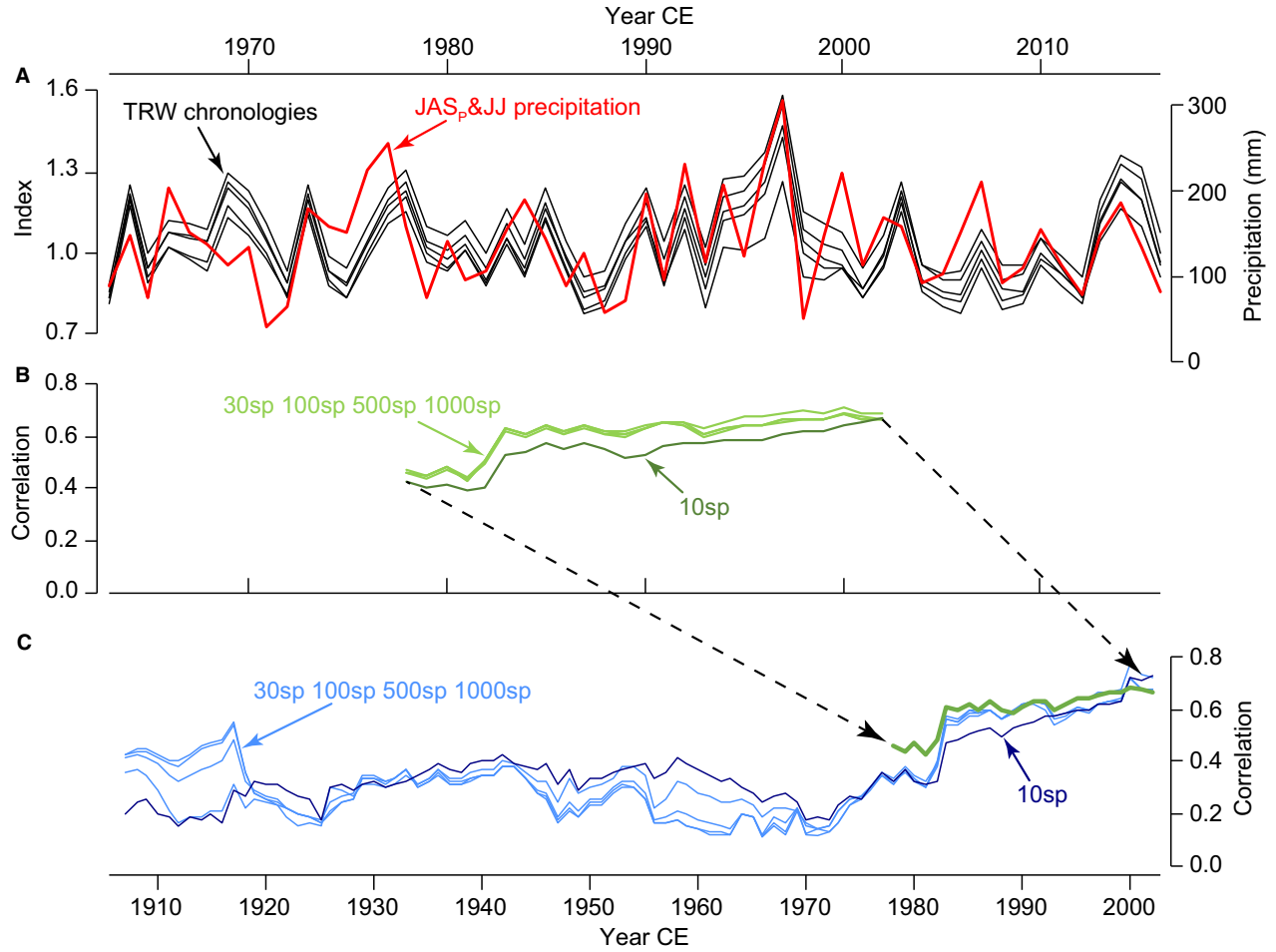

Fig. 8. Precipitation signal. A. Differently detrended CHEPI chronologies (black curves) shown together with precipitation totals from previous-year June–September and current-year June–July (JAS$_P$&JJ) recorded at three Corsican meteorological stations since 1962 CE (red). B. 30-year running correlations between the JAS$_P$&JJ precipitation record and 30sp, 100sp, 500sp and 1000sp (light green) and 10sp chronologies (dark green) from panel (A). C. The mean of the running correlations from panel (B) (green) shown together with 30-year running correlations of the CHEPI chronologies with JAS$_P$&JJ GPCC precipitation data from a nearby grid point at 9.125E and 42.125N since 1891 CE. Results for the 30sp, 100sp, 500sp and 1000sp chronologies shown in light blue, and for the 10sp chronology in dark blue.

Similarly, CHEPI chronologies were compared with previous-year September (Sep$_P$) PDSI over a shorter (1947–2016 CE) and longer period (1901–2016 CE) covered by local instrumental and gridded data, respectively (Fig. 9). We highlighted 1947–2016 CE in this second assessment as this period is continuously represented by one Corsican temperature station (Bastia at 10 m a.s.l.), whereas the earlier PDSI data are weighted towards remote stations within 450–1200 km search-radii (van der Schrier *et al.* 2013).

Both comparisons reveal significant correlations ($p < 0.01$) over the recent periods covered by regional meteorological station data. JAS$_P$&JJ precipitation correlates between $r_{1962–2016} = 0.56$ and 0.59 with the differently detrended CHEPI chronologies, though the running correlations include a drop in the early 1980s (green curves in Fig. 8B) largely driven by mismatching values in the late 1960s (red and black curves in Fig. 8). The 10sp CHEPI chronology persistently more weakly with target precipitation data indicating a loss of signal strength compared to its chronology counterparts that were detrended using stiffer splines (30sp–1000sp). All values drop below $r = 0.4$ before the 1980s when the 30-year running correlations extend over earlier periods represented by remote meteorological stations. This drop highlights the importance of considering local observational data for proxy calibration, even if these data include low-elevation stations that are weak predictors of the moist conditions at the tree line. The comparison with gridded GPCC precipitation data also shows increasing correlations to values >0.4 before the 1920s (except for 10sp and 30sp) pointing to some lower frequency, yet insignificant, proxy-target coherence.

Sep$_P$ PDSI correlates from $r_{1947–2016} = 0.38–0.53$ with the differently detrended CHEPI chronologies including a drop in the late 1970s when mismatching values in 1990

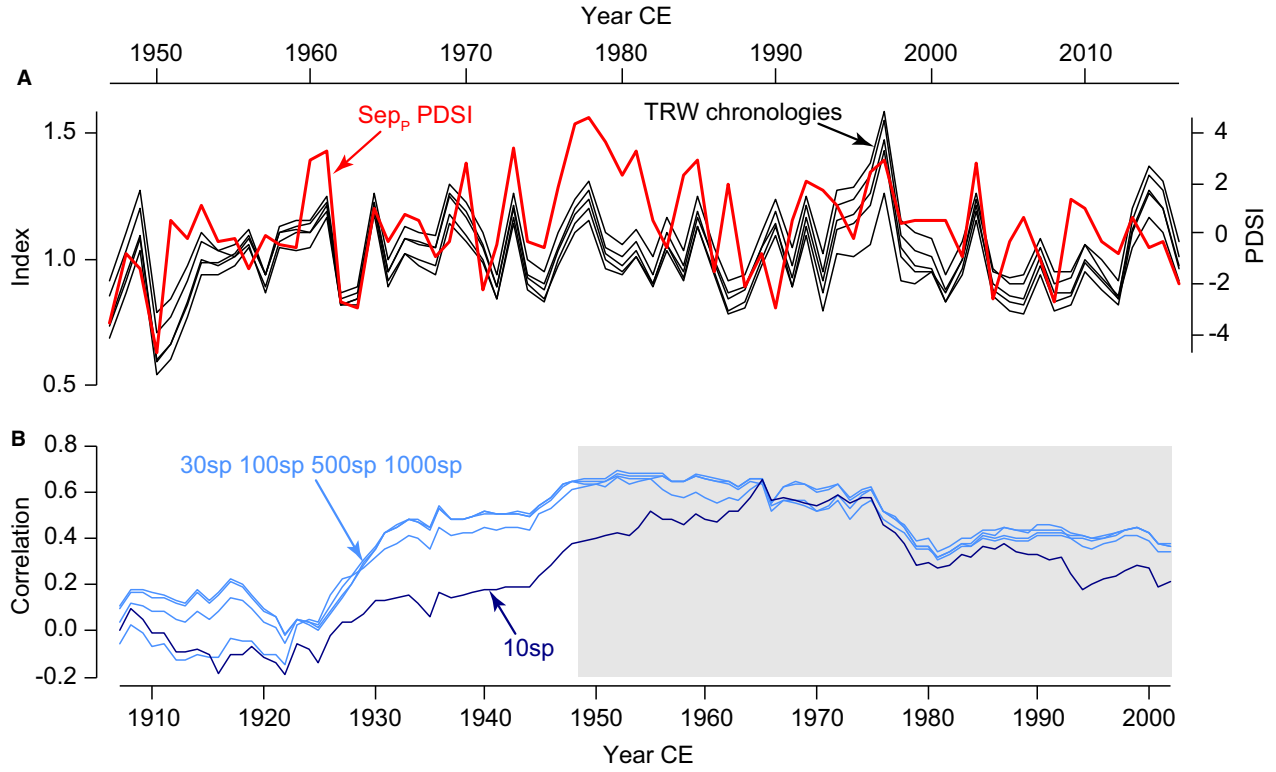

Fig. 9. PDSI signal. A. Differently detrended CHEPI chronologies (black curves) shown together with previous-year September PDSI (red; grid point at 9.125E, 42.125N) from 1947–2016 CE. B. 30-year running correlations between the PDSI record and 30sp, 100sp, 500sp and 1000sp (light blue) and 10sp chronologies (dark blue) from 1901–2016 CE. Grey box highlights the 1947–2016 CE period from panel (A).

and 1991 are included in the 30-year running correlations (Fig. 9). As with the precipitation readings, the 10sp CHEPI chronology correlates overall more weakly with PDSI, suggesting that climatically meaningful low frequency variance has been removed from this rigorously highpass-filtered record. Considering the extended 20th century period, the proxy-target correlations mostly remain >0.4 back to the 1930s (except for 10sp CHEPI), and then drop to values fluctuating around zero before the 1920s. This temporally extended correlation (back to the 1930s), compared to the TRW-vs.-precipitation results that already weaken before the 1980s (Fig. 8), likely results from the integration of temperature data into the PDSI as an important driver of evapotranspiration (van der Schrier *et al.* 2013). This interpretation considers the much longer correlation decay distances of temperature, compared to precipitation (Hofstra & New 2009; Büntgen *et al.* 2010b; Harris *et al.* 2020). Yet also temperature data become increasingly rare before the 1930s, even though the 1200-km search radius used in the PDSI grid includes meteorological stations on the Italian and French mainlands.

Reconstructions

Since it remains difficult to differentiate between precipitation and PDSI as the leading forcing controlling Corsican sub-alpine pine TRW variability, we produced millennium-length reconstructions for both climate variables (Fig. 10). The rigorously highpass-filtered 10sp CHEPI chronology was not included in these reconstructions as this time series was shown to contain weaker climate signals. However, lag-1 autocorrelations of the remaining CHEPI chronologies (30sp–1000sp) exceed the values of the instrumental target data (Esper *et al.* 2015b), except for 30sp vs. PDSI (Fig. S5), revealing uncertainty in reconstructed high-to-low frequency variance. These differences are not further assessed, or even adjusted, as the period of overlap with skilful observational data is too short and low frequency variance is coherent among Corsican pine high-elevation site chronologies (Fig. 4).

The scaled and smoothed 30sp–1000sp chronologies, as well as the interannual variability of the 1000sp version superimposed on these time series (Fig. 10), reveal rich high-to-low frequency precipitation and drought variability back to 974 CE. This variability is within the envelop of variance displayed by instrumental data since the mid 20th century. The reconstructions calibrate and verify at RE = 0.16–0.45 and CE = 0.08–0.40 for JAS$_P$&JJ precipitation, and RE = −0.32–0.27 and CE = −0.33–0.27 for Sep$_P$ PDSI (Table S1). These relatively low scores, including negative values when regressing CHEPI chronologies over early 1947–1981

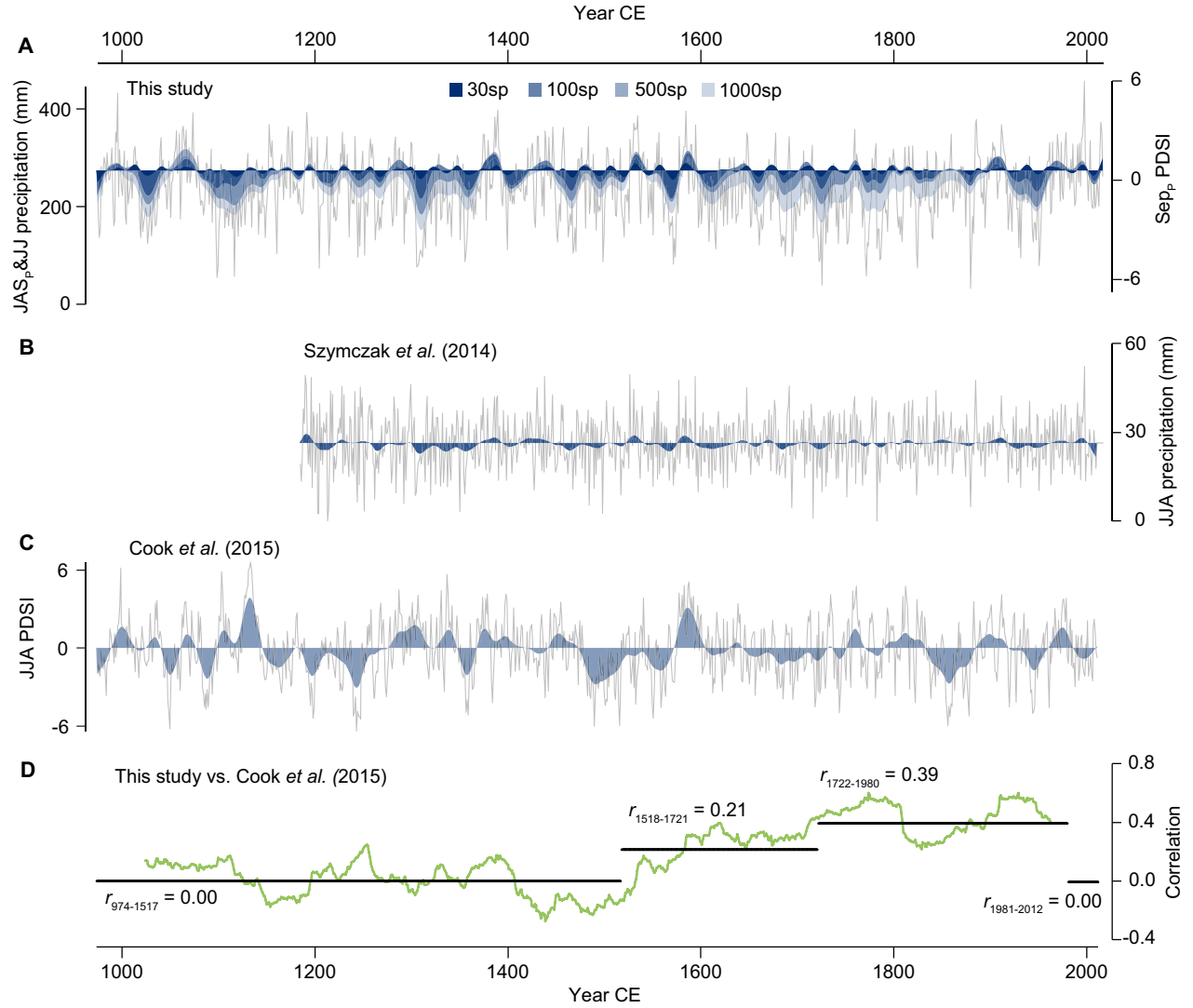

Fig. 10. Reconstructions and benchmarking. A. Hydroclimate reconstructions from 974–2016 CE derived from scaling the 1000sp CHEPI chronology (grey curve) against JAS$_P$&JJ precipitation (left axis) and Sep$_P$ PDSI data (right axis). Blue shadings indicate 30-year lowpass filters of the scaled 1000sp, 500sp, 100sp and 30sp CHEPI chronologies. B. JJA precipitation reconstruction from a Corsican pine network from 1185–2009 CE (grey curve) and its 30-year lowpass filter (blue) from Szymczak *et al.* (2014). C. JJA PDSI reconstruction (grid point at 9.125E and 42.125N) from 974–2012 CE (grey curve) and its 30-year lowpass filter (blue) from Cook *et al.* (2015). D. 100-year running correlations (green curve) between the PDSI reconstructions from this study and Cook *et al.* (2015). The horizontal lines mark the correlations over distinct periods: from 974–1517 and 1981–2012 CE when no Corsican predictor is included in Cook *et al.* (2015), from 1518–1721 CE when the Corsican predictor chronology is weakly replicated (<10 TRW series), and from 1722–1980 CE when the Corsican predictor chronology is well replicated (≥10 TRW series).

PDSI data, are likely affected by the short correlation decay distances and steep elevational gradients of precipitation data, constraining the skill of these statistical measures. However, there is no substantial drift in proxy-target residuals as expressed by DW values ranging from 1.67–1.71 and 1.51–1.60 for precipitation and PDSI, respectively.

Exceptionally moist and dry 30-year periods are reconstructed from 1051–1080, 1372–1401, 1518–1547 CE and 1013–1042, 1296–1325, 1711–1740 CE, when the transferred 1000sp chronology deviated >300 mm (>1.4 PDSI) and <180 mm (<−2.2 PDSI), respectively (Table S2). These periods and the reconstructed absolute values change, if other CHEPI chronologies are considered (see changing colours in Fig. 10A). The most extreme years/seasons include 1997 CE (458 mm, 6.0 PDSI), 995 CE (433 mm, 5.3 PDSI) and 1389 CE (398 mm, 4.3 PDSI), as well as 1879 CE (33 mm, −6.5 PDSI), 1725 CE (40 mm, −6.3 PDSI) and 1098 CE (56 mm, −5.9 PDSI); yet again absolute precipitation and PDSI deviations vary among the differently detrended CHEPI chronologies (Table S3). The reconstructions produced here are likely skilful back to 1150 and 974 CE until when the records exceed EPS

values of 0.9 and 0.8, respectively (Fig. S6). The 30sp CHEPI chronology includes a brief period centred around 1050 CE during which EPS drops to 0.79.

The precipitation reconstructions presented here extend previous attempts by more than 200 years (Fig. 10B) and provide additional information on decadal to multidecadal dry and moist periods. The coherent trends among site chronologies and robust climate correlations of the 1000sp CHEPI chronology argue for the use of this record to reconstruct multidecadal to centennial scale variability since 974 CE. Some of the lower frequency deviations reconstructed over the past 3–5 centuries are similar to a Corsican grid point reconstruction from the European drought atlas including moist periods from 1580–1600 and 1890–1920 CE, and dry periods from 1835–1875 and 1935–1960 CE (Fig. 10C). However, the significant correlations between our data and the PDSI grid point record gradually diminish back in time and fluctuate around zero before 1518 CE (as well as after 1980 CE; Fig. 10D). This pattern is linked to the period covered by a Corsican high-elevation pine chronology developed in the early 1980s and included as a predictor in the European drought atlas (Schweingruber & Briffa 1996). This chronology includes 29 TRW series in the late 19th century, but replication gradually declines before 1800, as is mirrored by the running correlation curve shown in green in Fig. 10D. The weakening, and gradually disappearing correlations reinforce the importance (i) of the number of measurement series (radii) included in a tree-ring chronology as a key metric of long-term reconstruction skill (Esper *et al*. 2016, 2018; Ljungqvist *et al*. 2020), and (ii) of local predictors in large-scale gridded networks of palaeoclimate variability. The next nearest predictors included in the European drought atlas are a *Larix decidua* chronology from the French Maritime Alps, a *Pinus uncinata* chronology from the Spanish Pyrenees, and a *Pinus heldreichii* chronology from southern Italy (Cook *et al*. 2015).

Conclusions

A well-replicated network of *Pinus nigra* TRW data from four Corsican mountain valleys has been developed to reconstruct high-to-low frequency hydroclimate variability over the past millennium. TRW site chronologies from this network correlate remarkably well over almost six centuries ($r_{1434–2016} = 0.70$) revealing climate variability to be a key forcing of Corsican sub-alpine tree growth. Attributing this signal to a particular climate parameter and season remains challenging, as the local meteorological stations do not represent the conditions at the upper tree line. This limitation is particularly striking for precipitation and derived drought parameters that are characterized by short correlation decay distances and dramatic changes along elevational transects in mountainous environments. We therefore conclude that the statistics obtained from calibrating sub-alpine TRW chronologies against (low-elevation) meteorological station data, ranging from $r_{1962–2016} = 0.59$ for precipitation to $r_{1947–2016} = 0.53$ for PDSI, underestimate the actual strength of pine growth forcing. This uncertainty also adds to the difficulty of distinguishing between precipitation and drought as the key controlling factor of TRW variability, so that reconstructions of both JAS_P&JJ precipitation and Sep_P PDSI were produced. These time series are derived from scaling differently detrended pine chronologies against observational data to emphasize high-to-low frequency hydroclimate variability from 974–2016 CE. The new records extend previous attempts by more than 200 years and add multidecadal scale variability to existing estimates. Comparison with a millennium-length PDSI reconstruction from a European scale grid returned significant covariance only during the period covered by a local (Corsican) predictor chronology, but zero correlations before and thereafter. This assessment reinforces the need to develop more hydroclimate reconstructions covering the last millennium to support large-scale studies of pre-instrumental climate variability and forcing.

Acknowledgements. – Supported by the German Research Foundation (Grant No. ES 161/12-1), SustES (CZ.02.1.01/0.0/0.0/16_019/0000797) and ERC Advanced Grant Monostar (AdG 882727). The German Research Foundation supported C. Hartl (Grant No. HA 8048/1-1), S. Szymczak (Grant No. SZ 356/1-1) and A. Bräuning (Grant No. BR 1895/27-1). We are grateful to Yannik Esser, Christian Gnaneswaran, Markus Kochbeck, Benedikt Lang, Lea Schneider, Robin Schulz and Birgit Wöste for help in the field and laboratory.

Author contributions. – JE designed the study and developed the methodological framework, with contributions from CH, OK, FR, PR, FH, AB and UB. JE, CH, OK, FR, PR, FH, SL, SS and AB carried out fieldwork. JE conducted the analysis and wrote the paper, with support from PR, FH and UB. All authors discussed and revised the manuscript.

Data availability statement. – The reconstructions and underlying TRW series will be submitted to the International Tree Ring Databank (ITRDB).

References

Blasing, T. J., Duvick, D. N. & Cook, E. R. 1983: Filtering the effects of competition from ring-width series. *Tree-Ring Bulletin 43*, 19–30.

Briffa, K. R. 1984: *Tree-climate relationships and dendroclimatological reconstruction in the British Isles*. Ph.D. thesis, University of East Anglia, 285 pp.

Briffa, K. R., Jones, P. D., Bartholin, T. S., Eckstein, D., Schweingruber, F. H., Karlen, W., Zetterberg, P. & Eronen, M. 1992: Fennoscandian summers from AD 500: temperature changes on short and long timescales. *Climate Dynamics 7*, 111–119.

Briffa, K. R., Schweingruber, F. H., Jones, P. D., Osborn, T. J., Shiyatov, S. G. & Vaganov, E. A. 1998: Reduced sensitivity of recent tree-growth to temperature at high northern latitudes. *Nature 391*, 678–682.

Büntgen, U., Brázdil, R., Dobrovolný, P., Trnka, M. & Kyncl, T. 2011a: Five centuries of Southern Moravian drought variations revealed from living and historic tree rings. *Theoretical and Applied Climatology 105*, 167–180.

Büntgen, U., Raible, C. C., Frank, D., Helama, S., Cunningham, L., Hofer, D., Nievergelt, D., Verstege, A., Timonen, M., Stenseth, N. C. & Esper, J. 2011b: Causes and consequences of past and projected Scandinavian summer temperatures, 500–2100 AD. *PLoS One 6*, e25133, https://doi.org/10.1371/journal.pone.0025133.

Büntgen, U., Frank, D., Neuenschwander, T. & Esper, J. 2012: Fading temperature sensitivity of Alpine tree growth at its Mediterranean margin and associated effects on large-scale climate reconstructions. *Climatic Change 114*, 651–666.

Büntgen, U., Frank, D., Trouet, V. & Esper, J. 2010a: Diverse climate sensitivity of Mediterranean tree-ring width and density. *Trees 24*, 261–273.

Büntgen, U., Franke, J., Frank, D., Wilson, R., Gonzales-Rouco, F. & Esper, J. 2010b: Assessing the spatial signature of European climate reconstructions. *Climate Research 41*, 125–130.

Büntgen, U., Krusic, P. J., Verstege, A., Sangüesa-Barreda, G., Wagner, S., Camarero, J., Charpentier Ljungqvist, F., Zorita, E., Oppenheimer, C., Konter, O., Tegel, W., Gärtner, H., Cherubini, P., Reinig, F. & Esper, J. 2017: New tree-ring evidence from the Pyrenees reveals Western Mediterranean climate variability since medieval times. *Journal of Climate 30*, 5295–5318.

Carrer, M., Nola, P., Motta, R. & Urbinati, C. 2010: Contrasting tree-ring growth to climate responses of Abies alba toward the southern limit of its distribution area. *Oikos 119*, 1515–1525.

Castagneri, D., Nola, P., Motta, R. & Carrer, M. 2014: Summer climate variability over the last 250 years differently affected tree species radial growth in a mesic Fagus–Abies–Picea old-growth forest. *Forest Ecology and Management 320*, 21–29.

Cook, E. R. & Peters, K. 1981: The smoothing spline: a new approach to standardizing forest interior tree-ring width series for dendroclimatic studies. *Tree-Ring Bulletin 41*, 45–53.

Cook, E. & Peters, K. 1997: Calculating unbiased tree-ring indices for the study of climatic and environmental change. *The Holocene 7*, 361–370.

Cook, E. R., Briffa, K. R. & Jones, P. D. 1994: Spatial regression methods in dendroclimatology: a review and comparison of two techniques. *International Journal of Climatology 14*, 379–402.

Cook, E. R. and 57 others. 2015: Old World megadroughts and pluvials during the Common Era. *Science Advances 1*, e1500561, https://doi.org/10.1126/sciadv.1500561.

D'Arrigo, R., Wilson, R. & Jacoby, G. 2006: On the long-term context for late twentieth century warming. *Journal of Geophysical Research: Atmospheres 111*, D03103, https://doi.org/10.1029/2005JD006352.

Durbin, J. & Watson, G. S. 1951: Testing for serial correlation in least squares regression. II. *Biometrika 38*, 159–177.

Esper, J., Cook, E. R. & Schweingruber, F. H. 2002: Low-frequency signals in long tree-ring chronologies for reconstructing past temperature variability. *Science 295*, 2250–2253.

Esper, J., Düthorn, E., Krusic, P. J., Timonen, M. & Büntgen, U. 2014: Northern European summer temperature variations over the Common Era from integrated tree-ring density records. *Journal of Quaternary Science 29*, 487–494.

Esper, J., Frank, D., Büntgen, U., Verstege, A., Luterbacher, J. & Xoplaki, E. 2007: Long-term drought severity variations in Morocco. *Geophysical Research Letters 34*, L17702, https://doi.org/10.1029/2007GL030844.

Esper, J., Frank, D. C., Timonen, M., Zorita, E., Wilson, R. J. S., Luterbacher, J., Holzkämper, S., Fischer, N., Wagner, S., Nievergelt, D., Verstege, A. & Büntgen, U. 2012: Orbital forcing of tree-ring data. *Nature Climate Change 2*, 862–866.

Esper, J., Frank, D. C., Wilson, R. J. & Briffa, K. R. 2005: Effect of scaling and regression on reconstructed temperature amplitude for the past millennium. *Geophysical Research Letters 32*, L07711, https://doi.org/10.1029/2004GL021236.

Esper, J., Hartl, C., Tejedor, E., de Luis, M., Günther, B. & Büntgen, U. 2020a: High-resolution temperature variability reconstructed from Black pine tree ring densities in southern Spain. *Atmosphere 11*, 748, https://doi.org/10.3390/atmos11070748.

Esper, J., Klippel, L., Krusic, P. J., Konter, O., Raible, C. C., Xoplaki, E., Luterbacher, J. & Büntgen, U. 2020b: Eastern Mediterranean summer temperatures since 730 CE from Mt. Smolikas tree ring densities. *Climate Dynamics 54*, 1367–1382.

Esper, J., Konter, O., Klippel, L., Krusic, P. J. & Büntgen, U. 2021: Pre-instrumental summer precipitation variability in northwestern Greece from a high-elevation *Pinus heldreichii* network. *International Journal of Climatology 41*, 2828–2839.

Esper, J., Konter, O., Krusic, P., Saurer, M., Holzkämper, S. & Büntgen, U. 2015a: Long-term summer temperature variations in the Pyrenees from detrended stable carbon isotopes. *Geochronometria 42*, 53–59.

Esper, J., Schneider, L., Smerdon, J. E., Schöne, B. R. & Büntgen, U. 2015b: Signals and memory in tree-ring width and density data. *Dendrochronologia 35*, 62–70.

Esper, J., Krusic, P. J., Ljungqvist, F. C., Luterbacher, J., Carrer, M., Cook, E., Davi, N. K., Hartl-Meier, C., Kirdyanov, A., Konter, O., Myglan, V., Timonen, M., Treydte, K., Trouet, V., Villalba, R., Yang, B. & Büntgen, U. 2016: Ranking of tree-ring based temperature reconstructions of the past millennium. *Quaternary Science Reviews 145*, 134–151.

Esper, J., St. George, S., Anchukaitis, K., D'Arrigo, R., Ljungqvist, F., Luterbacher, J., Schneider, L., Stoffel, M., Wilson, R. & Büntgen, U. 2018: Large-scale, millennial-length temperature reconstructions from tree-rings. *Dendrochronologia 50*, 81–90.

Fang, K., Davi, N., Gou, X., Chen, F., Cook, E., Li, J. & D'Arrigo, R. 2010: Spatial drought reconstructions for central High Asia based on tree rings. *Climate Dynamics 35*, 941–951.

Frank, D. & Esper, J. 2005a: Characterization and climate response patterns of a high-elevation, multi-species tree-ring network in the European Alps. *Dendrochronologia 22*, 107–121.

Frank, D. & Esper, J. 2005b: Temperature reconstructions and comparisons with instrumental data from a tree-ring network for the European Alps. *International Journal of Climatology 25*, 1437–1454.

Frank, D., Esper, J. & Cook, E. R. 2007: Adjustment for proxy number and coherence in a large-scale temperature reconstruction. *Geophysical Research Letters 34*, L16709, https://doi.org/10.1029/2007GL030571.

Griggs, C., DeGaetano, A., Kuniholm, P. & Newton, M. 2007: A regional high-frequency reconstruction of May–June precipitation in the north Aegean from oak tree rings, A.D. 1089–1989. *International Journal of Climatology 27*, 1075–1089.

Harris, I., Osborn, T. J., Jones, P. & Lister, D. 2020: Version 4 of the CRU TS monthly high-resolution gridded multivariate climate dataset. *Scientific Data 7*, 109, https://doi.org/10.1038/s41597-020-0453-3.

Hartl, C., Düthorn, E., Tejedor, E., Kirchhefer, A. J., Timonen, M., Holzkämper, S., Büntgen, U. & Esper, J. 2021: Micro-site conditions affect Fennoscandian forest growth. *Dendrochronologia 65*, 125787, https://doi.org/10.1016/j.dendro.2020.125787.

Häusser, M., Szymczak, S., Garel, E., Santoni, S., Huneau, F. & Bräuning, A. 2019: Growth variability of two native pine species on Corsica as a function of elevation. *Dendrochronologia 54*, 49–55.

Hellmann, L., Agafonov, L., Ljungqvist, F. C., Churakova, O., Düthorn, E., Esper, J., Hülsmann, L., Kirdyanov, A. V., Moiseev, P., Myglan, V. S., Nikolaev, A. N., Reinig, F., Schweingruber, F. H., Solomina, O., Tegel, W. & Büntgen, U. 2016: Diverse growth trends and climate responses across Eurasia's boreal forest. *Environmental Research Letters 11*, 074021, https://doi.org/10.1088/1748-9326/11/7/074021.

Hetzer, T. 2013: *Xylem variability as a proxy for environmental and climate change in Corsica during the past millennium*. Ph.D. thesis, Friedrich-Alexander-University, 208 pp.

Hofstra, N. & New, M. 2009: Spatial variability in correlation decay distance and influence on angular-distance weighting interpolation of daily precipitation over Europe. *International Journal of Climatology 29*, 1872–1880.

Holmes, R. L. 1983: Computer-assisted quality control in tree-ring dating and measurement. *Tree-Ring Bulletin 43*, 69–78.

Klesse, S., Ziehmer, M., Rousakis, G., Trouet, V. & Frank, D. 2015: Synoptic drivers of 400 years of summer temperature and precipitation variability on Mt. Olympus, Greece. *Climate Dynamics 45*, 807–824.

Klippel, L., Krusic, P. J., Brandes, R., Hartl, C., Belmecheri, S., Dienst, M. & Esper, J. 2018: A 1286-year hydro-climate reconstruction for the Balkan Peninsula. *Boreas 47*, 1218–1229.

Klippel, L., Krusic, P. J., Konter, O., St. George, S., Trouet, V. & Esper, J. 2019: A 1200+ year reconstruction of temperature extremes for the

northeastern Mediterranean region. *International Journal of Climatology 39*, 2336–2350.
Knerr, I., Trachte, K., Garel, E., Huneau, F., Santoni, S. & Bendix, J. 2020: Partitioning of large-scale and local-scale precipitation events by means of spatio-temporal precipitation regimes on Corsica. *Atmosphere 11*, 417, https://doi.org/10.3390/atmos11040417.
Lebourgeois, F., Mérian, P., Courdier, F., Ladier, J. & Dreyfus, P. 2012: Instability of climate signal in tree-ring width in Mediterranean mountains: a multi-species analysis. *Trees 26*, 715–729.
Leonelli, G., Coppola, A., Salvatore, M. C., Baroni, C., Battipaglia, G., Gentilesca, T., Ripullone, F., Borghetti, M., Conte, E., Tognetti, R., Marchetti, M., Lombardi, F., Brunetti, M., Maugeri, M., Pelfini, M., Cherubini, P., Provenzale, A. & Maggi, V. 2017: Climate signals in a multispecies tree–ring network from central and southern Italy and reconstruction of the late summer temperatures since the early 1700s. *Climate of the Past 13*, 1451–1471.
Ljungqvist, F. C., Piermattei, A., Seim, A., Krusic, P. J., Büntgen, U., He, M., Kirdyanov, A., Luterbacher, J., Schneider, L., Seftigen, K., Stahle, D., Villalba, R., Yang, B. & Esper, J. 2020: Ranking of tree-ring based hydroclimate reconstructions of the past millennium. *Quaternary Science Reviews 230*, 106074, https://doi.org/10.1016/j.quascirev.2019.106074.
Luterbacher, J. and 33 others 2012: A review of 2000 years of paleoclimatic evidence in the Mediterranean. *In* Lionello, P. (ed.): *The climate of the Mediterranean region: From the Past to the Future*, 87–185. Elsevier, Amsterdam.
Römer, P., Hartl, C., Schneider, L., Bräuning, A., Szymczak, S., Huneau, F., Lebre, S., Reinig, F., Büntgen, U. & Esper, J. 2021: Reduced temperature sensitivity of maximum latewood density formation in high-elevation Corsican pines under recent warming. *Atmosphere 12*, 804, https://doi.org/10.3390/atmos12070804.
Schneider, L., Esper, J., Timonen, M. & Büntgen, U. 2014: Detection and evaluation of an early divergence problem in northern Fennoscandian tree-ring data. *Oikos 123*, 559–566.
Schneider, U., Finger, P., Rustemeier, E., Ziese, M. & Becker, A. 2021: *Global Precipitation Analysis Products of the GPCC*. 15 pp. Deutscher Wetterdienst, Offenbach.
van der Schrier, G., Barichivich, J., Briffa, K. R. & Jones, P. D. 2013: A scPDSI-based global data set of dry and wet spells for 1901–2009. *Journal of Geophysical Research: Atmospheres 118*, 4025–4048.
Schweingruber, F. H. & Briffa, K. R. 1996: Tree-ring density networks for climate reconstruction. *In* Jones, P. D., Bradley, R. S. & Jouzel, J. (eds.): *Climatic Variations and Forcing Mechanisms of the Last 2000 Years*, 43–66. Springer, Berlin.
Seim, A., Büntgen, U., Fonti, P., Haska, H., Herzig, F., Tegel, W., Trouet, V. & Treydte, K. 2012: Climate sensitivity of a millennium-long pine chronology from Albania. *Climate Research 51*, 217–228.
Seim, A., Treydte, K., Trouet, V., Frank, D., Fonti, P., Tegel, W., Panayotov, M., Fernández-Donado, L., Krusic, P. & Büntgen, U. 2015: Climate sensitivity of Mediterranean pine growth reveals distinct east-west dipole. *International Journal of Climatology 35*, 2503–2513.
Szymczak, S., Bräuning, A., Häusser, M., Garel, E., Huneau, F. & Santoni, S. 2019: The relationship between climate and the intra-annual oxygen isotope patterns from pine trees: a case study along an elevation gradient on Corsica, France. *Annals of Forest Science 76*, 1–14.
Szymczak, S., Bräuning, A., Häusser, M., Garel, E., Huneau, F. & Santoni, S. 2020a: A dendroecological fire history for Central Corsica/France. *Tree-Ring Research 76*, 40–53.
Szymczak, S., Häusser, M., Garel, E., Santoni, S., Huneau, F., Knerr, I., Trachte, K., Bendix, J. & Bräuning, A. 2020b: How do Mediterranean pine trees respond to drought and precipitation events along an elevation gradient? *Forests 11*, 758, https://doi.org/10.3390/f11070758.
Szymczak, S., Hetzer, T., Bräuning, A., Joachimski, M. M., Leuschner, H. H. & Kuhlemann, J. 2014: Combining wood anatomy and stable isotope variations in a 600-year multi-parameter climate reconstruction from Corsican black pine. *Quaternary Science Reviews 101*, 146–158.
Szymczak, S., Joachimski, M. M., Bräuning, A., Hetzer, T. & Kuhlemann, J. 2012: A 560 yr summer temperature reconstruction for the Western Mediterranean basin based on stable carbon isotopes from *Pinus nigra* ssp. *laricio* (Corsica/France). *Climate of the Past 8*, 1737–1749.
Tejedor, E., de Luis, M., Cuadrat, J. M., Esper, J. & Saz, M. A. 2016: Tree-ring-based drought reconstruction in the Iberian Range (east of Spain) since 1694. *International Journal of Biometeorology 60*, 361–372.
Tejedor, E., Saz, M. Á., Cuadrat, J. M., Esper, J. & Luis, M. D. 2017a: Temperature variability in the Iberian Range since 1602 inferred from tree-ring records. *Climate of the Past 13*, 93–105.
Tejedor, E., Saz, M. A., Esper, J., Cuadrat, J. M. & de Luis, M. 2017b: Summer drought reconstruction in northeastern Spain inferred from a tree ring latewood network since 1734. *Geophysical Research Letters 44*, 8492–8500.
Trouet, V. 2014: A tree-ring based late summer temperature reconstruction (AD 1675–1980) for the northeastern Mediterranean. *Radiocarbon 56*, 69–78.
Wigley, T. M. L., Briffa, K. R. & Jones, P. D. 1984: On the average of correlated time series, with applications in dendroclimatology and hydrometeorology. *Journal of Applied Meteorology and Climate 23*, 201–213.

Supporting Information

Additional Supporting Information may be found in the online version of this article at http://www.boreas.dk.

Table S1. Verification statistics of the 30sp–1000sp CHEPI chronologies regressed against JAS_P&JJ precipitation (top) and Sep_P PDSI (bottom) over the full, late and early calibration periods.

Table S2. Reconstructed JAS_P&JJ precipitation and Sep_P PDSI derived from scaled 30sp–1000sp CHEPI chronologies. Top (bottom) panel shows three wettest (driest) 30-year periods of each reconstruction.

Table S3. Reconstructed JAS_P&JJ precipitation and Sep_P PDSI derived from scaled 30sp–1000sp CHEPI chronologies. Top (bottom) panel shows 10 wettest (driest) seasons of each reconstruction.

Fig. S1. Age-aligned tree-ring data. A. Arithmetic mean curves of the age-aligned TRW series from Asco, Ballone, Golo and Tartagine shown together with (B) site replication curves.

Fig. S2. Climate data correlation fields. A. Correlation of the ABC_T station mean combining temperatures from Ajaccio, Bastia and Calacuccia with CRU 4.04 January (left panel) and July temperatures (right panel) from 1962–2016. B. Same as in (A), but for local PDSI data (grid point at 9.25E and 42.25N) and GPCC precipitation. C. Same as in (B), but for local PDSI vs. CRU temperatures.

Fig. S3. Power spectra of the 10sp, 30sp, 100sp, 500sp and 1000sp detrended CHEPI chronologies.

Fig. S4. Pearson vs. Spearman correlations. A. Pearson correlations of the differently detrended CHEPI

chronologies (colours) with monthly mean precipitation totals of the Ajaccio, Bastia and Calacuccia stations (ABC_P) from 1962–2016. Results from previous-year March (M_P) to current-year October (O) are shown. B. Same as in (A), but using Spearman rank correlations. C. Monthly residuals from calculating Spearman minus Pearson correlations.

Fig. S5. Lag-1 autocorrelations of the spline detrended CHEPI chronologies (10sp–1000sp), September PDSI (9.25E/42.25N), JAS_P&JJ station and GPCC precipitation records (9.125E/42.125N) from 1962–2016 (green), 1947–2016 (grey) and 1901–2016 (blue). Note that the station precipitation record extends back to only 1962.

Fig. S6. Rbar (A) and EPS (B) statistics of the differently detrended CHEPI chronologies (30sp–1000sp) calculated over 50-year periods shifted in 25-year steps along the past millennium.